Electronic Supplementary Information for

Exceeding the Volcano Relationship in Oxygen Reduction/Evolution Reactions using Single-atom-based Catalysts with Dual-active-sites

Xiyu Li,[a†] Sai Duan,[b†] Edward Sharman,[c] Yuan Zhao,[a] Li Yang,[a] Zhiwen Zhuo,[a] Peng Cui,[a] Jun Jiang*[a] and Yi Luo.

[a] Hefei National Laboratory for Physical Sciences at the Microscale, Collaborative Innovation Center of Chemistry for Energy Materials, School of Chemistry and Materials Science, University of Science and Technology of China, Hefei, Anhui 230026, P. R. China

[b] Collaborative Innovation Center of Chemistry for Energy Materials, Shanghai Key Laboratory of Molecular Catalysis and Innovative Materials, MOE Key Laboratory of Computational Physical Sciences, Department of Chemistry, Fudan University, Shanghai 200433, P. R. China

[c] Department of Neurology, University of California, Irvine, California 92697, USA

Corresponding author. E-mail: jiangj1@ustc.edu.cn

Computational DFT method and CHE model details

DFT method

All calculations were carried out at the spin-polarized density functional theory (DFT) level using the VASP package. The Kohn–Sham equations of the valence electrons were expanded using plane-wave basis sets. The Perdew, Burke, and Ernzerhof (PBE) exchange-correlation functional within a generalized gradient approximation (GGA) and the projector augmented-wave (PAW) potential were employed. [1-4] The energy cutoff was set to 500 eV. 1×1×1 Monkhorst-Pack k-meshes were used for molecular systems. Structure relaxation is stopped once the force on each atom is less than 0.02 eV/Å. The climbing-image nudged elastic band (CI-NEB) method with implicit solvent effect was used to calculate activation energy barriers.

CHE (computational hydrogen electrode) model

In the electrochemical process, the hydrogen evolution reaction mechanism can be described as:

$$H^+(aq) + e^- \rightarrow 1/2H_2\,(g) \qquad (1)$$

The free enregies of G_{H2}, G_{H+} and G_{e-} can be definied as:

$$G_{H2}=(G_{H2})_0 + k_BTln[P_{H2}/P_0] \qquad (2)$$

$$G_{H+}= (G_{H+})_0 - \Delta G_{pH} = (G_{H+})_0 + k_BTln[H^+] =(G_{H+})_0 - pH\times k_BTln10 \qquad (3)$$

$$G_{e-}= (G_{e-})_0 + (-e_0)U \qquad (4)$$

where U is the electrode applied potential (*vs.* reversible hydorgen electrode, RHE); k_B is the Boltzmann constant, T is the temperature, P_{H2} is the H_2 gas pressure, e_0 is the elementary charge. $(G_{H2})_0$, $(G_{H+})_0$ and $(G_{e-})_0$ are the free energies of H_2, $H^+$and e^- under standard condiction (pH=0, $P_{H2} = P_0$ =1 bar, T = 298 K, U=0).

Under standard condiction, the hydrogen evolution reaction is reversible ($H^+(aq) + e^- \rightleftharpoons 1/2H_2(g)$) and the free energy difference of Eq. 1 is zero eV, which can be discribed as:

$$\Delta G = 0 =1/2(G_{H2})_0 - [(G_{H+})_0 + (G_{e-})_0]$$

This means the free energy of proton-electron pair is equal to that of half a hydrogen molecule. This technique is the so-called computational hydrogen eletrode (CHE) model, which allow us to obtain the free energy of proton-electron pair.

To obtain the reaction free energy of each elementary step of ORR/OER, we can calculate the adsorption free energies of OOH, O and OH intermediates. Since it is difficult to obtain the accurare free energies of OOH, O and OH radicals in the electrolyte solution, the adsorption free energy ΔG_{OOH}, ΔG_O and ΔG_{OH} are relative to the free energy of stoichiometrically appropriate amounts of H_2O (g) and H_2 (g).

It is known that the high-spin ground state of the oxygen molecule is poorly described in DFT calculations. Accroding to total free energy difference of the ORR/OER process $\{O_2\,(g) + 4[H^+(aq) + e^-] \rightarrow 2H_2O\,(l) \rightleftharpoons 2H_2O\,(g)\}$, the free energy of the O_2 molecule can derived according to $G_{O2}\,(g) = 2G_{H2O}\,(l) - 2G_{H2}\,(g) + 4 \times 1.23$ (eV). The free energy of $(OH^- - e^-)$was derived as $G_{OH-} - (G_{e-}) = G_{H2O}\,(l) - [G_{H+(aq)} + (G_{e-})]$. The free energy for gas phase water is calculated at 0.035 bars because this is the equilibrium pressure in contact with liquid water at 298 K. The free energy of gas phase water at these conditions is equal to the free energy of liquid water.

For each elementary step, the Gibbs reaction free energy (ΔG) is defined as the difference between free energies of the initial and final states and is given by the expression:

$$\Delta G=\Delta E + \Delta ZPE - T\Delta S + \Delta G_U + \Delta G_{pH}$$

where ΔE is the reaction energy of reactant and product molecules adsorbed on catalyst surface, which can be obtained from DFT calculations; ΔZPE and ΔS are the change in zero point energies and entropy at 298 K.

The bias effect on the free energy of each initial, intermediate and final state involving an electron in the electrode is taken into account by shifting the energy of the state by $\Delta G_U = - ne_0U$, where n is the number of proton–electron pairs transferred. The effect of basic/acidic condition (pH effect) on thermodynamics is described by ΔG_{pH} ($\Delta G_{pH} = -k_BTln[H+] = pH\times k_BTln10$).

Therefore, we can calculate the free energy change of ΔG_{*O}, ΔG_{*OH} and ΔG_{*OOH} :

$\Delta G_{*O} = \Delta G[H_2O(g) + * \rightarrow *O + H_2(g)] = (E_{*O} + E_{H2} - E_{H2O} - E_*) + (E_{ZPE-*O} + E_{ZPE-H2} - E_{ZPE-H2O} - E_{ZPE-*}) - T\times(S_{*O} + S_{H2} - S_{H2O} - S_*)$;

$\Delta G_{*OH} = \Delta G[H_2O(g) + * \rightarrow *OH + 1/2H_2(g)] = (E_{*OH} + 0.5\times E_{H2} - E_{H2O} - E_*) + (E_{ZPE-*OH} + 0.5\times E_{ZPE-H2} - E_{ZPE-H2O} - E_{ZPE-*}) - T\times(S_{*OH} + 0.5\times S_{H2} - S_{H2O} - S_*)$;

$\Delta G_{*OOH} = \Delta G[2H_2O(g) + * \rightarrow *OOH + 3/2H_2(g)] = (E_{*OOH} + 1.5\times E_{H2} - 2\times E_{H2O} - E_*) + (E_{ZPE-*OOH} + 1.5\times E_{ZPE-H2} - 2\times E_{ZPE-H2O} - E_{ZPE-*}) - T\times(S_{*OOH} + 1.5\times S_{H2} - 2\times S_{H2O} - S_*)$;

The OER free energy profile of single-active-site can be calculated by the following equations:

(1) $OH^- + * \rightarrow *OH + e^-$; $\Delta G_{1\text{-}OER} = \Delta G_{*OH}$
(2) $*OH + OH^- \rightarrow *O + H_2O + e^-$; $\Delta G_{2\text{-}OER} = \Delta G_{*O} - \Delta G_{*OH}$
(3) $*O + OH^- \rightarrow *OOH + e^-$; $\Delta G_{3\text{-}OER} = \Delta G_{*OOH} - \Delta G_{*O}$
(4) $*OOH + OH^- \rightarrow * + O2 + H_2O + e^-$; $\Delta G_{4\text{-}OER} = 4.92 - \Delta G_{*OOH}$

The OER free energy profile of dual-active-site can be calculated by the following equations:

(1) $OH^- + * \rightarrow *OH + e^-$; $\Delta G_{1\text{-}OER} = \Delta G_{*OH}$
(2) $OH^- + * \rightarrow *OH + e^-$; $\Delta G_{2\text{-}OER} = \Delta G_{*OH}$
(3) $*OH + OH^- \rightarrow *O + H_2O + e^-$; $\Delta G_{3\text{-}OER} = \Delta G_{*O} - \Delta G_{*OH}$
(4) $*OH + OH^- \rightarrow *O + H_2O + e^-$; $\Delta G_{4\text{-}OER} = \Delta G_{*O} - \Delta G_{*OH}$
(5) $*O + *O \rightarrow 2* + O_2$; $\Delta G_{5\text{-}OER} = 4.92 - \Delta G_{*OOH} = 4.92 - 2\Delta G_{*O}$

The overpotential (η) is calculated by:

$$\eta = [\max(\Delta G_{i\text{-}OER}) - 1.23\ eV\ ]/e$$

The ORR free energy profile of single-active-site can be calculated by the following equations:

(1) $O_2 + * + H_2O + e^- \rightarrow *OOH + OH^-$; $\Delta G_{1\text{-}ORR} = - (4.92 - \Delta G_{*OOH})$
(2) $*OOH + e^- \rightarrow *O + OH^-$; $\Delta G_{2\text{-}ORR} = - (\Delta G_{*OOH} - \Delta G_{*O})$
(3) $*O + H_2O + e^- \rightarrow *OH + OH^-$; $\Delta G_{3\text{-}ORR} = - (\Delta G_{*O} - \Delta G_{*OH})$
(4) $*OH + e^- \rightarrow OH^- + *$; $\Delta G_{4\text{-}ORR} = - (\Delta G_{*OH})$

The ORR free energy profile of dual-active-sites can be calculated by the following equations:

(1) $O_2 + * + H_2O + e^- \rightarrow *OOH* + OH^-$; $\Delta G_{1\text{-}ORR} = - (4.92 - \Delta G_{*OOH})$

(2) $*OOH* \rightarrow *O + *OH$; $\Delta G_{2\text{-}ORR} = - (\Delta G_{*OOH} - \Delta G_{*O} + \Delta G_{*OH})$

(3) $*O + H_2O + e^- + *OH \rightarrow *OH + OH^- + *OH$; $\Delta G_{3\text{-}ORR} = - (\Delta G_{*O} - \Delta G_{*OH})$

(4) $*OH + e^- + *OH \rightarrow OH^- + * + *OH$; $\Delta G_{4\text{-}ORR} = - (\Delta G_{*OH})$

(5) $OH^- + * + *OH + e^- \rightarrow 2OH^- + 2*$; $\Delta G_{5\text{-}ORR} = - (\Delta G_{*OH})$

The limiting-potential (U_L) calculated by:

$$U_L = -[\min(\Delta G_{i\text{-}ORR})]/e$$

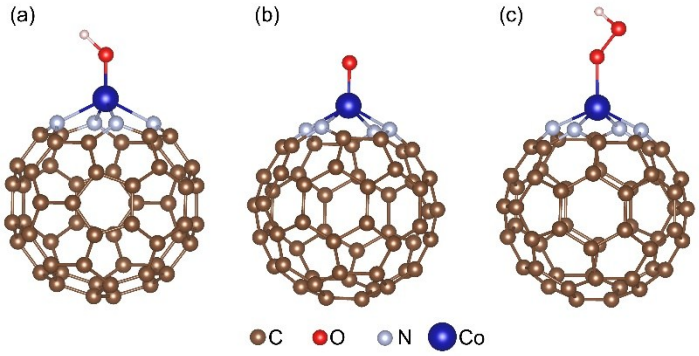

Figure S1 Atomic structures of OH (a), O (b) and OOH (c), bound to the CoN_4-C_{60} catalyst.

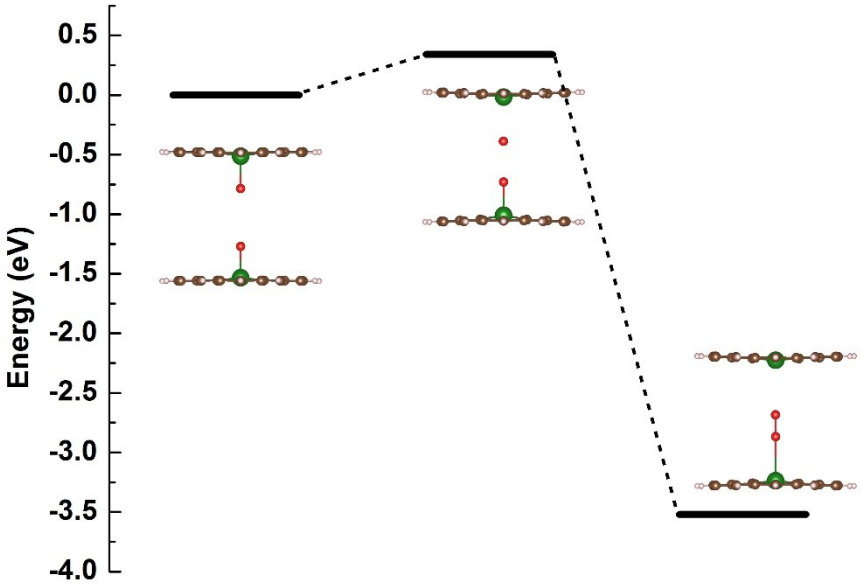

Figure S2 The activation energy with the implicit solvent effect for molecular oxygen formation by the reverse of Eq. 5 catalyst with dual-active-site of ZnC_4. The green ball stands for Zn atom.

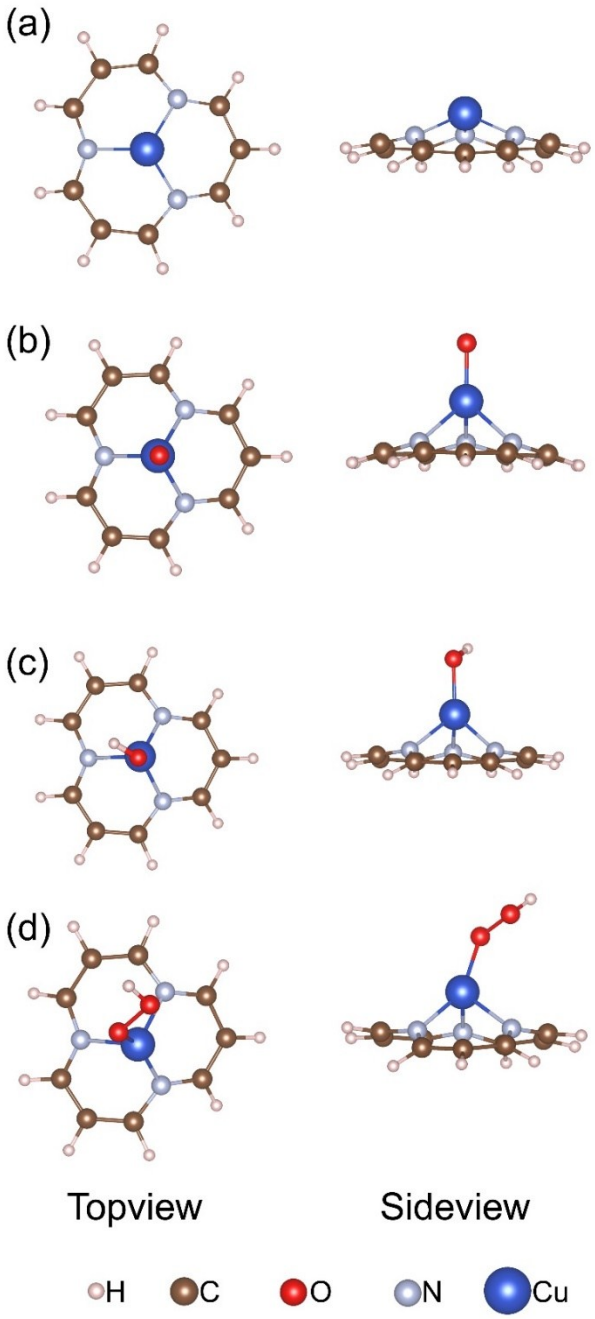

Figure S3 Atomic structures of CuN_3 (a), and of CuN_3 with the adsorbed ORR intermediates *O (b), *OH (c) and *OOH (d) viewed from the top and side.

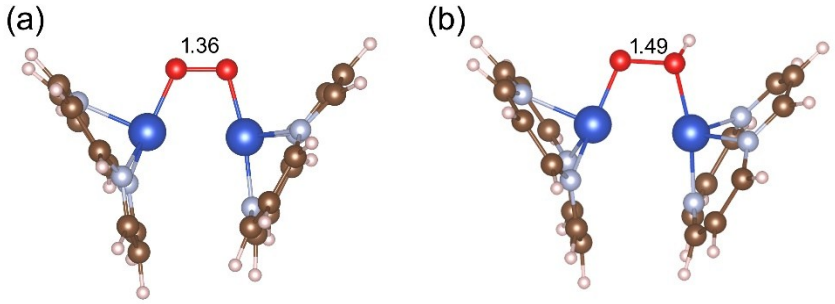

Figure S4 Atomic structures of *OO* (a) and *OOH* (b) bound to Cu-SV-3N with dual-activity-sites. Figure S4a shows the most stable *OO* structure, in which the O-O bond length is 1.36 Å and each O atom is bound to a catalyst monomer. The reaction energy for the dissociation of *OO* into two separate species *O and *O is 1.61 eV, indicating that the activation energy of this dissociation would be above 1.61 eV and thus dissociation would be impossible at low-temperatures.

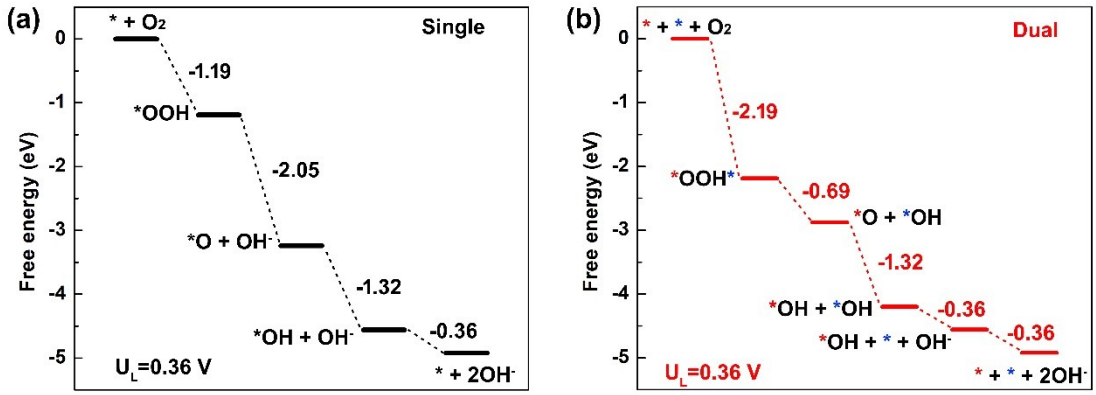

Figure S5 ORR free energy profiles for single-active-site (a) and dual-active-site (b) of NiN_3.

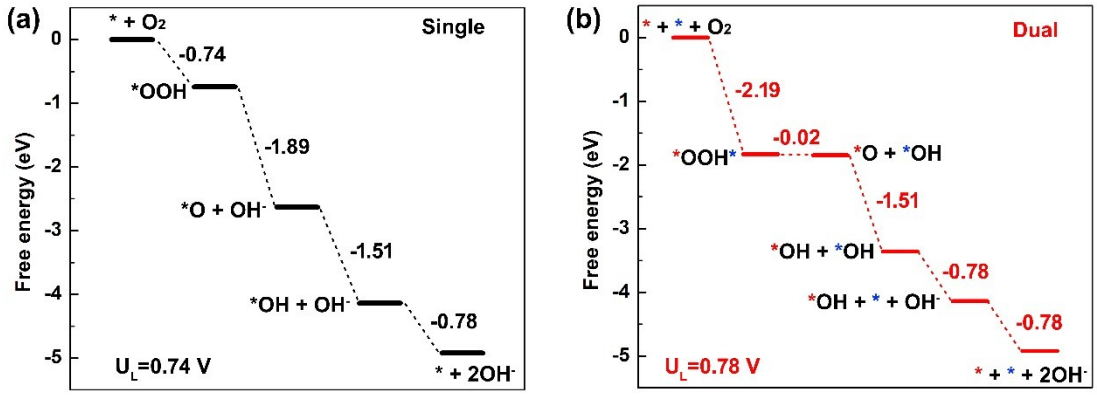

Figure S6 ORR free energy profiles for single-active-site (a) and dual-active-site (b) of ZnN_3.

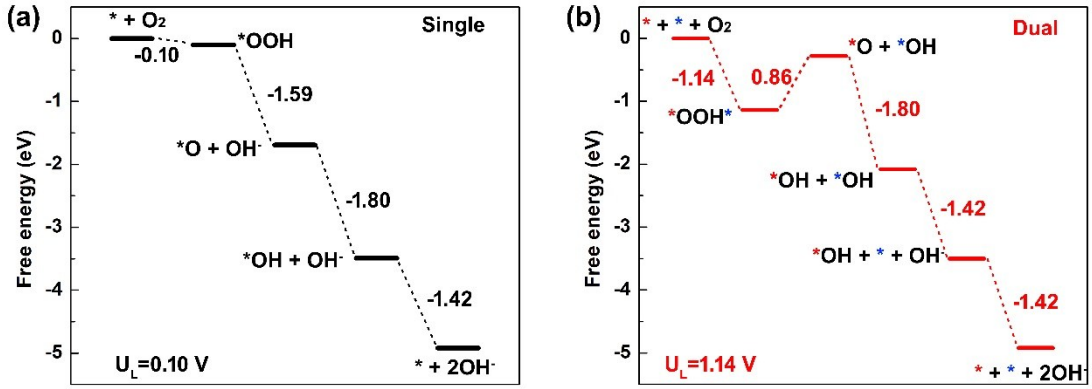

Figure S7 ORR free energy profiles for single-active-site (a) and dual-active-site (b) of AgN_3.

Discussion of the results shown in Figure S5-S7

Specifically, for Ni-macrocycle complexes with a single-active-site (shown in Figure S5), the PDS (potential-determining step) is OH^- formation (Eq. 4). This differs from the PDS of Cu-SV-3N with a single-active-site (OOH* formation). Replacement with a dual-active-site in Ni-macrocycle complexes doesn't change either the PDS and U_L. As another example, the respective free energy profiles of Zn–macrocycle complexes with single- and dual-active-sites are shown in Figure S6. Here one can see that the PDS is Eq. 1 and U_L is 0.74 V for this catalyst with a single-active-site; for a dual-active-site instead, its PDS is Eq. 4 and the U_L is 0.78 V. For Ag-SV-3N with a single-active-site (Figure S7), the PDS is Eq. 1 and U_L is 0.10 V, due to the weak binding energy of *OOH. In the case of a dual-active-site, the PDS is still Eq. 1, but the value of U_L is 1.14 V, due to the strong binding energy of *OOH*, which is very close to the ideal value. Nevertheless, the free energy barrier of Eq. 8 is as high as 0.86 eV, which indicates that the activation energy of this process is higher than 0.86 eV and the reaction rate of this step would be slow at low temperature. As an alternative, protonation of *OOH* (*OOH* + H^+ + e^- → *OH + *OH) with a free energy difference of -0.96 eV can be realized, and the corresponding U_L is 0.96 V in this situation. Based on these results, one discovers that, only when *OOH formation is the PDS (weak OOH binding) at a single-active-site, can the dual-active-site form *OOH* with stronger OOH binding as a result of the additional dimension of interaction, changing both the PDS and the value of U_L. If *OOH formation is not the PDS for the single-active-site, the dual-active-site would not be able to change the PDS and U_L of ORR, which results from the fact that the dual-active-site can bind *OOH* more strongly without affecting the binding energy of *OH or *O.

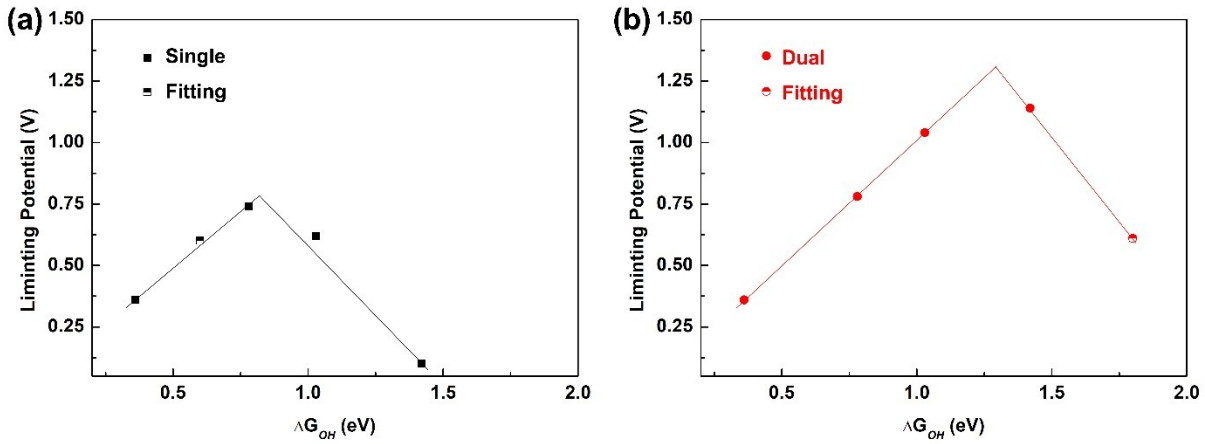

Figure S8 Volcano plots of ORR active trends for single-active-site (a) and dual-active-sites (b), which are based on the calculations of single-active-site and dual-active-sites. The fitting dots can be obtained from the scaling relationships between *OOH and *OH are $\Delta G_{OOH} = \Delta G_{OH} + 3.36$ eV (single-active-site) and $\Delta G_{OOH} = \Delta G_{OH} + 2.41$ eV (dual-active-sites), respectively.

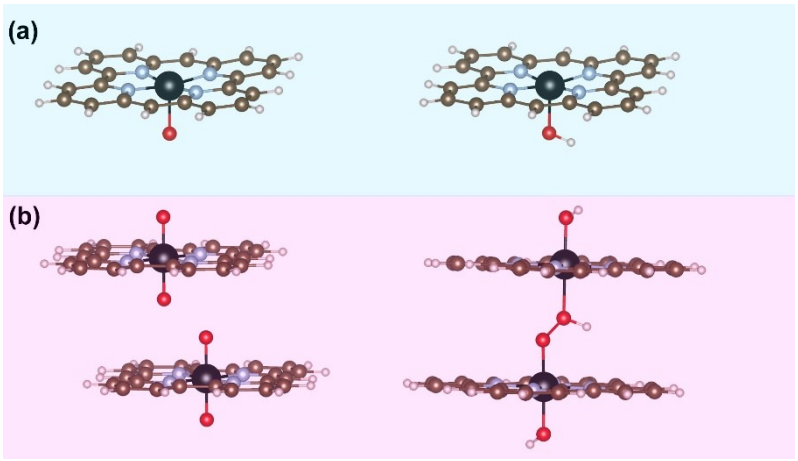

Figure S9 The atomic structures of metal-macrocycle complexes with active site of $TMN_4(O)$ for OER and $TMN_4(OH)$ for ORR (a) and the atomic structures of dual-active-sites of $TMN_4(O)$ with two adsorbed *O to form oxygen molecule along OER pathway and the *OOH* adsorbed on dual-active-sites of $TMN_4(OH)$ along ORR pathway (b).

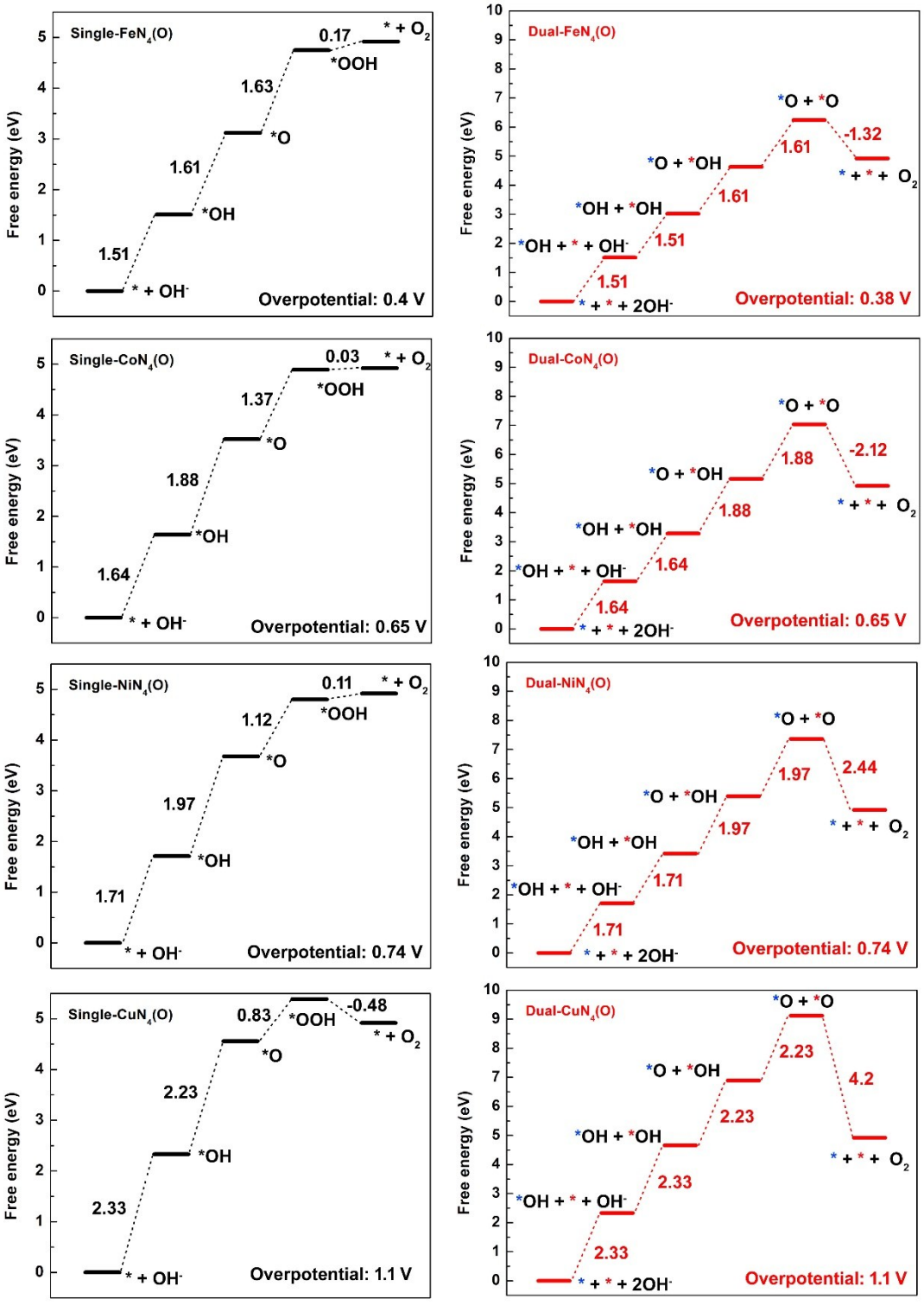

Figure S10 The calculated OER free energy profiles for single-active-site and dual-active-sites of $TMN_4(O)$. For the single-active-site of $TMN_4(O)$, the lowest overpotential is 0.4 V on FeN4(O). The potential-determining step is the *OOH formation (reversal of Eq.2). In the case of dual-active-sites of $TMN_4(O)$, the lowest overpotential is 0.38 V on FeN4(O) and the potential-determining step is the *O formation (reversal of Eq.3). Nevertheless, in the case of Co/Ni/$CuN_4(O)$ dual-active-sites, the overpotential is not lower than that of single-active-site. It is because the dual-active-sites cannot promote reactions if the *OOH formation step is not the potential-determining step.

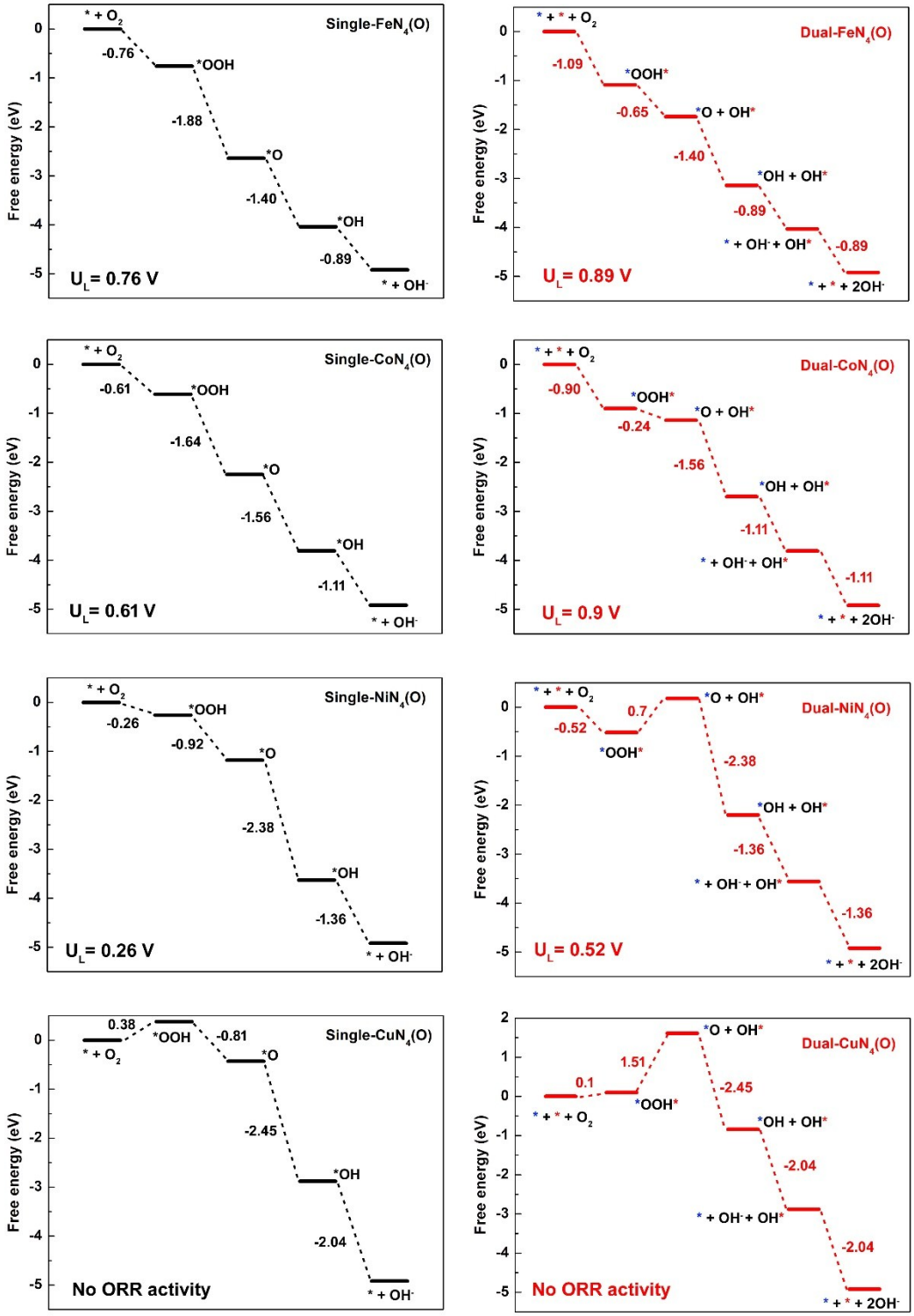

Figure S11 The calculated ORR free energy profiles for single-active-site and dual-active-sites of $TMN_4(OH)$. For ORR catalyzed by the $TMN_4(OH)$ single-active-site, the limiting-potential step is the *OOH formation. The binding energy of *OOH* is stronger than that of *OOH. As a result, the limiting-potential of $TMN_4(OH)$ single-active-site can be improved by changing to dual-active-sites. Specifically, the limiting-potential of $FeN_4(OH)$ is improved from 0.76 with single-active-site to 0.89 V with dual-active-sites. For $CoN_4(OH)$, the limiting-potential is improved from 0.61 to 0.90 V. For $NiN_4(OH)$, the limiting-potential is improved from 0.26 to 0.52 V.

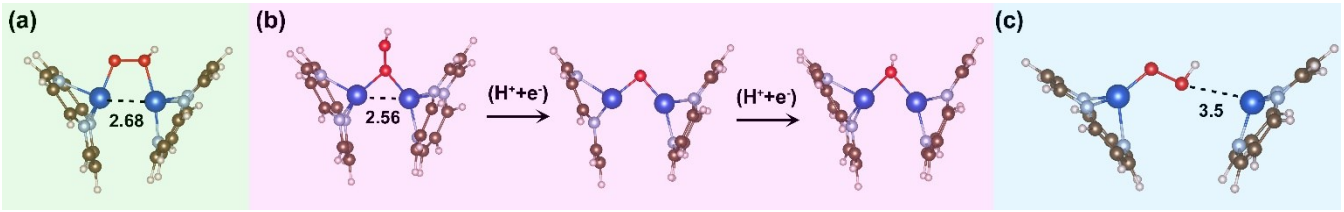

Figure S12 Structures of *OOH* (a), *O*OH, *O* and *OH* (b), and *OOH + * (c), which are determined by the distance (in Angstroms) between the two Cu metal atoms in Cu- macrocycle complexes dual-active-site. The blue, red, and pink balls represent metal, oxygen, hydrogen atoms, respectively.

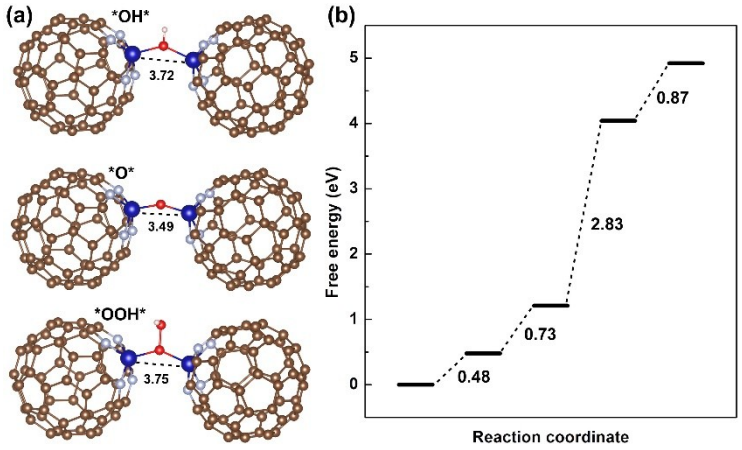

Figure S13 (a) The atomic structures of *O*H, *O*, and *O*OH *OH* with short Co-Co distance (in Angstroms), and (b) the corresponding OER free energy profile. The blue, red, and pink balls represent cobalt metal, oxygen, hydrogen atoms, respectively.

From the view of thermodynamics, simulations of the CoN_4 molecular SAC for OER, and of Ni/Cu/Zn/AgN_3 molecular SACs for ORR demonstrate that the strategy of designing catalysts with dual-active-site is an effective method for optimizing catalytic activity. Admittedly, the distance between two single-active-sites is a key factor for determining whether the steps of the reverse of Eq. 5 and 8 can be realized. For instance, Figure S12a shows a structure in which the two O atoms in *OOH* are bound to two Cu atoms that are separated by a Cu-Cu distance of 2.68 Å. The -OOH intermediate can also be adsorbed on these two Cu atoms by the binding of only one O atom (*O*OH) with a Cu-Cu distance of 2.56 Å (Figure S12b). Once this adsorption configuration is formed, *O* or *OH* would be produced by reduction. However, the binding energy of *OH* is so strong that the calculated free energy difference for the *OH* reduction step is only 0.05 eV, implying that the ORR catalytic activity would be poor in the case of such a short distance. If the distance between these two Cu atoms is so large that *OOH is out of reach of the second active site and consequently cannot interact with it (Figure S12c), the situation reverts to that of Cu-SV-3N with a single-active-site. As a result, a suitable distance between these two single-active-sites is key to realizing formation of *OOH* in ORR as well as in the reverse Eq. 5 process for OER. When the Co-Co distance is 3.75 Å, the intermediates can be bound to the two Co atoms to form *OH*, *O* and *OOH*. In this case, it is a single-active-site with two Co atoms involved for OER. The calculated free energy profile shows that the overpotential is 1.5 V due to the *OOH* formation step, implying poor OER activity. Once the Co-Co distance is large enough (longer than 5.75 Å), it could be turned back into the scene of two isolated single-active-sites with overpotential of 1.04 V. The Co-Co distance of dual-active-sites with optimized OER activity (overpotential of 0.08 V) is at the range of 3.75 ~ 5.75 Å.

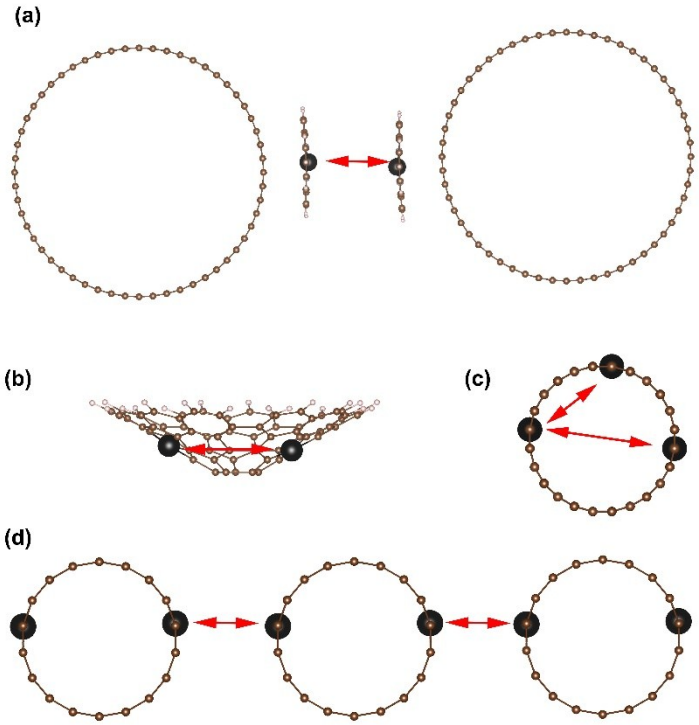

Figure S14 Schemes of dual-active-sites based on carbon materials. In experiment, dual-active-sites can be constructed by two adjacent single-active-sites with the help of particular confinements of carbon materials. As Figure S14, the dual-active-sites can also be constructed by two separate catalysts with single-active-site which can adsorbe on walls of two nanotubes by strong chemical bonds or π–π stacking interaction. The dual-active-sites can also perpared by doping TM into specific carboncone and carbon nanotube.

Table S1 The difference between ΔG_{OOH} and ΔG_{OH} in the works of Ref. 27, 28, 29.

	ΔG_{OOH} - ΔG_{OH} (eV)	η (V)
Ref.27	2.94	0.26
Ref.28	2.75	0.2
Ref.29	2.53	0.18

Table S2 The effect of distance between two Co metal atoms (Co-Co distance) on the OER activities.

OER		
Co-Co distance (Å)	Active site	Overpotential(V)
shorter than the sum of two Co-O chemical bond-lengths (<3.75)	One single-active-site	1.5
3.75 ~ 5.75	Dual-active-sites	0.08
longer than the sum of two Co-O chemical bond-lengths and 2 Å (> 5.75)	Two single-active-site	1.04

Reference

(1) P. E. Blochl, Phys. Rev. B 50, 17953 (1994).

(2) G. Kresse and J. Furthm€uller, Phys. Rev. B 54, 11169 (1996).

(3) G. Kresse and D. Joubert, Phys. Rev. B 59, 1758 (1999).

(4) J. P. Perdew, K. Burke, and M. Ernzerhof, Phys. Rev. Lett. 77, 3865 (1996).